

Clotilde Corsi

Far-Field Optimisation of Heliostat Shape and Spacings

Clotilde Corsi, Victor Grigoriev, Manuel Blanco

CSIRO Energy Centre, 10 Murray Dwyer Circuit, Mayfield West, NSW 2304, Australia

E-mail: clotilde.corsi@csiro.au

Abstract

A better efficiency of heliostat field implies a denser layout, but shading and blocking losses impose limits on how close heliostats can be deployed. These limits can be analysed by modelling and simulating the optical behaviour of a small group of heliostats arranged on a lattice with adjustable azimuthal and radial spacings. The optimal spacings are found by maximising the annual effective area efficiency of a heliostat for a given mirror density. This approach is used to evaluate heliostats of different tracking types and aspect ratios. The results obtained shows that tilt-and-roll heliostats of landscape orientation improve annual effective surface efficiency.

1. Introduction

Solar tower power plants with storage have a number of benefits for commercialisation and became a subject of extensive development in recent years (Lovegrove and Stein, 2012). The receiver on top of the tower collects light from a large field of heliostat mirrors which rotate automatically to track the motion of the sun. In general, the cost of constructing the heliostat field is about 40% of the total cost of the plant (Coventry and Pye, 2014). Because of this, even a small improvement in the heliostat field layout may result in considerable savings.

The efficiency of a heliostat field is determined by several factors (Stine and Geyer, 2001), which are not equally important for optimisation. The reflectivity of the mirrors is a constant which is usually fixed. The atmospheric attenuation factor depends on the distance from the heliostat to the target. The cosine and spillage factors depend on the motion of the sun, and their annual values can be precomputed for any position in the field. The actual layout of a heliostat field, which sets the limit on the mirror density, is determined mainly by the desire to minimise shading and blocking losses.

In this work, a model for analysing the shading and blocking losses in a small group of heliostats is developed. It is used to evaluate heliostats of different tracking types and aspect ratios locally instead of considering the full heliostat field. This approach is not only faster, but it also helps to clarify what is optimal for different parts of the field.

This paper provides details of the model (Section 2) by describing how to compute the shading and blocking losses via parallel projection and polygon clipping. This includes how to place a heliostat in a group based on a lattice pattern. The results of the optimisation for heliostats of different tracking types and aspect ratios are presented and discussed (Section 3).

2. Calculation of shading and blocking losses

2.1. Parallel projection and polygon clipping

The shading and blocking losses can be computed via parallel projections in the direction of the sun and tower, respectively [Figure 1]. The small angular distribution of sun rays (Buie et al., 2003) can be neglected for short distances between heliostats (Ramos and Ramos, 2014). If heliostats are sufficiently close to one another, their normals \mathbf{n} do not differ much (Collado and Guallar, 2012), and the projected offsets are $\mathbf{p} = \mathbf{r} - q\mathbf{s}$, where $q = (\mathbf{r} \cdot \mathbf{n}) / (\mathbf{s} \cdot \mathbf{n})$ as can be checked by requiring $\mathbf{p} \cdot \mathbf{n} = 0$. If $q < 0$ the projected heliostat is located behind and can be excluded from consideration. The projection in the blocking direction can be done in a similar way. After projections, a polygon clipping algorithm (Agoston, 2005) is applied to determine the effective area of the mirror, i.e. the area that is neither blocked or shadowed. The scanline algorithm of Vatti was selected because it is numerically stable.

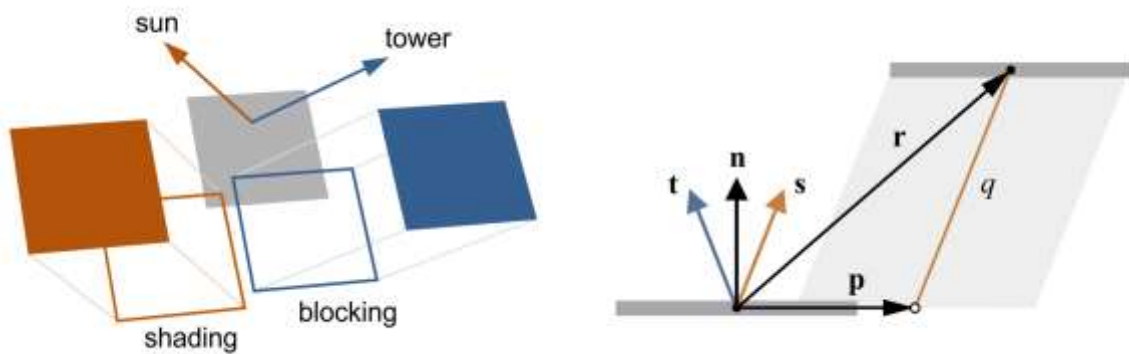


Figure 1. Calculation of shading and blocking via parallel projection.

2.2. Heliostat group

It is more important to minimise the blocking losses, because they always happen in a fixed direction to the tower. This justifies the radial design of heliostat fields. The shading losses are minimised by increasing the space between heliostats, which can be achieved by adding a radial shift [Figure 2].

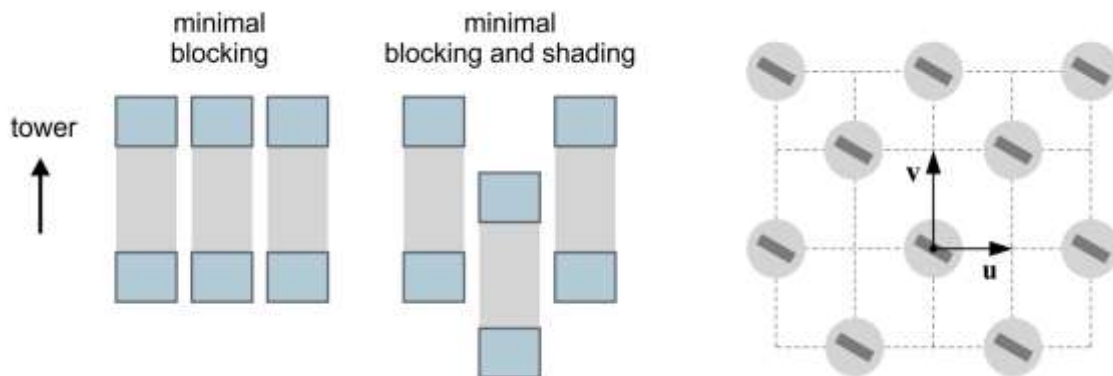


Figure 2. Radial stagger layout as a lattice.

It is sufficient to analyse the annual shading and blocking in a small group of heliostats rather than in the full field. For instance, a total number of 40 neighbouring heliostats limit the error to 1% for the examples presented in Section 3. The position of such a group in the field can be parameterised using the azimuth γ_t and elevation α_t of the target vector. At far distances from the tower (relative to the size of heliostats), the radial curvature can be neglected and the resulting layout resembles a periodic lattice. This approximation will be called as far-field, and it should be appropriate for scanning a large set of parameters. The coordinates of the heliostats in the group can be described as

$$\mathbf{r}_{ij} = i\mathbf{u} + j\mathbf{v}, \quad (1)$$

where \mathbf{u} and \mathbf{v} are the lattice vectors, and only the nodes with even $i + j$ are filled. The lattice layout have been also used to analyse the shading losses in arrays of sun-tracking collectors (Cumpston and Pye, 2014). The local mirror density (Lipps and Vant-Hull, 1978) for rectangular mirrors of the width w and height h can be defined as

$$f = \frac{wh}{2uv}. \quad (2)$$

As an example, the tilt-roll heliostats of square shape can be considered. Figure 3 shows how the shading and blocking losses are computed in this case. Additional views are provided in Figure 4. It is worth noting that the shading and blocking areas can overlap, and the corresponding losses should be considered as a single term. For convenience, the analysis of shading and blocking is described by the instantaneous heliostat area efficiency, η_v , defined by the ratio between the effective and total area of a heliostat.

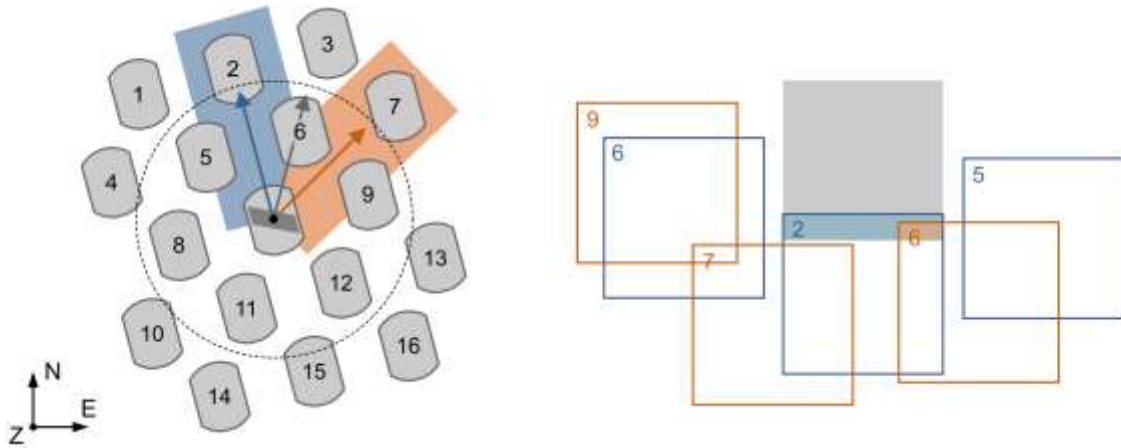


Figure 3. Top view of heliostat group (a) and projections of neighbours on the central heliostat (b).

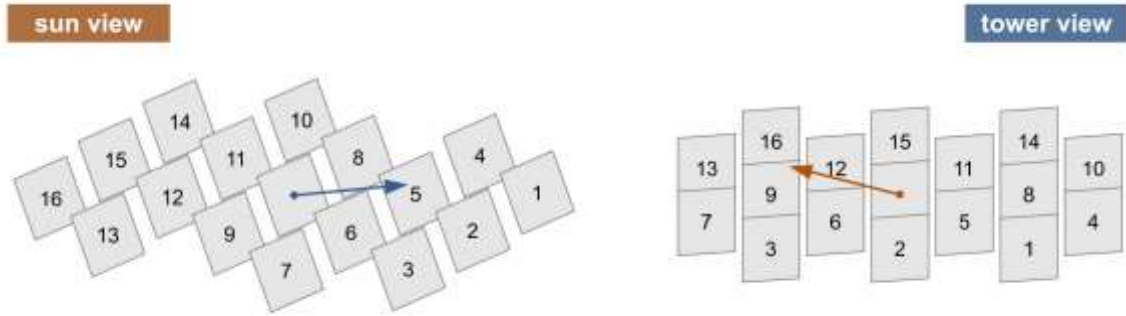


Figure 4. Heliostat group viewed from the sun (a) and tower (b).

2.3. Estimation of azimuthal and radial spacings

The optimal spacings can be estimated by using a nonblocking condition (Collado and Turégano, 1989). In the simplest case, when the sun and tower have the same azimuth, it follows from Figure 5 that

$$2v \frac{\sin \alpha_t}{\cos \theta} \geq h, \quad (3)$$

As a result, the blocking can be excluded if the radial separation is chosen as

$$v = \frac{h}{2 \sin \alpha_t}. \quad (4)$$

The azimuthal separation can be estimated in a similar way by using top view (Siala and Elayeb, 2001), which gives

$$u = w. \quad (5)$$

The corresponding mirror density is $f_m = \sin \alpha_t$ as can be checked by substituting Eqs. (4) and (5) into Eq. (2).

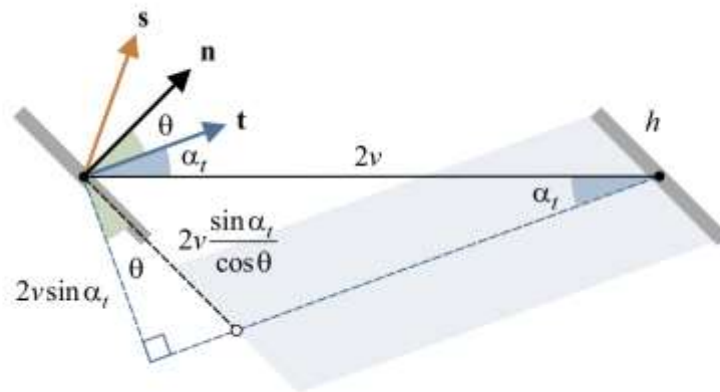


Figure 5. Estimation of nonblocking separation in a side view.

3. Optimisation of mirror density

The derivation of heliostat spacings (4) and (5) is based on a number of strong assumptions which may be questionable in different parts of the field (Al-Rabghi and Elsayed, 1991). Moreover, it is not possible to tell how strong the mirror density depends on shading and blocking. As a consequence, there is no flexibility for balancing between density and efficiency, which is a key for the design of dense heliostat fields. The model developed for a small heliostat group proves to be very useful in this regard, because the required data can be extracted numerically.

The annual effective area efficiency $\bar{\eta}_v$ of heliostat is defined as a weighted average of the instantaneous effective area efficiency η_v

$$\bar{\eta}_v = \frac{\int_{\text{year}} \eta_v I \cos \theta dt}{\int_{\text{year}} I \cos \theta dt}, \quad (6)$$

where I is the direct normal irradiance, and θ is the angle of incidence. The annual integration can be replaced by a sum

$$\bar{\eta}_v = \frac{\sum_p w_p [\eta_v \cos \theta](\mathbf{s}_p)}{\sum_p w_p [\cos \theta](\mathbf{s}_p)}, \quad (7)$$

where the sampling points \mathbf{s}_p and their weights w_p are selected in a special way to maximise the accuracy (Grigoriev et al., 2015).

3.1. Comparison of azimuth-elevation and tilt-roll heliostats

The annual effective surface efficiency can be computed as a function of azimuthal and radial separations in the heliostat group. The optimisation of lattice parameters is much simpler and faster than an iterative placement of heliostats based on shading maps (Yao et al., 2015). As an example, the heliostats of different tracking types are compared in **Error! Reference source not found.** The heliostats are of square shape with the width and height equal to 10 m. The aiming direction of the group has the azimuth 0° and elevation 20° . The collision envelope (Schramek and Mills, 2004) is shown as an empty area in the corner. It has the shape of sphere (barrel) for tracking in azimuth-elevation (tilt-roll). The contours of a fixed mirror density are shown by thick lines, and the maximal mirror density for a given annual effective surface efficiency is marked by dots. The estimated spacings (4) and (5) are shown as dashed lines.

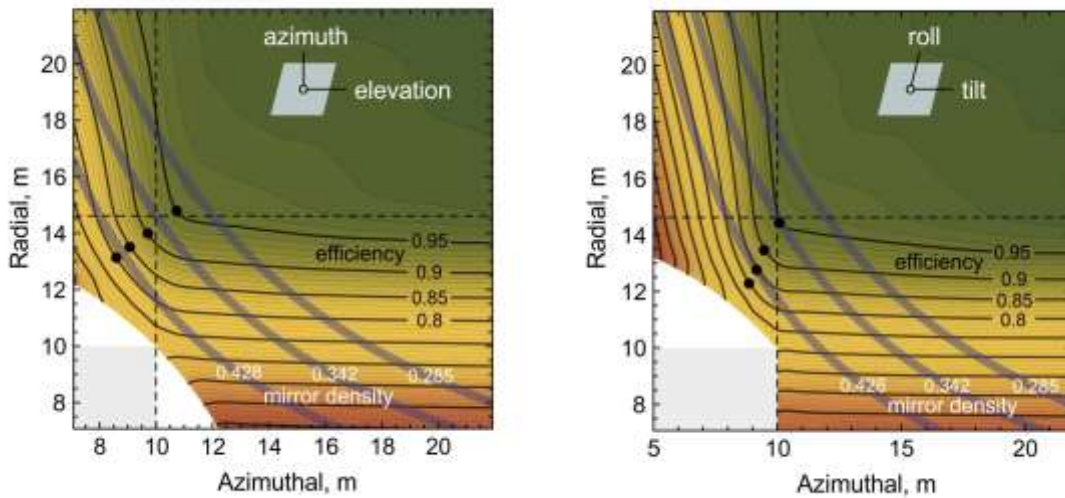


Figure 6. Annual effective heliostat area efficiency as a function of azimuthal and radial separations for azimuth-elevation (a) and tilt-roll tracking (b).

It can be noticed that the estimations are quite accurate in this case. The annual effective surface efficiency is nearly a constant within the nonblocking area and sharply drops outside it. The collision envelope does not play a major role for the given position in the field. However, the tilt-roll heliostats perform slightly better than the azimuth-elevation ones. The maximal mirror density is plotted as a function of the annual effective surface efficiency [Figure 7], which shows the improvements more clearly. They can be interpreted in terms of either annual effective surface efficiency (2%) or mirror density which can be achieved for the same effective mirror efficiency (8%). The latter can be very important for placing more heliostats in a high efficiency area. A similar behaviour is observed not only in the south of the tower, but also in the north of it. The improvement grows even further in this case. It also highlights the fact that concentric rings may not be optimal for the placement of heliostats around the tower.

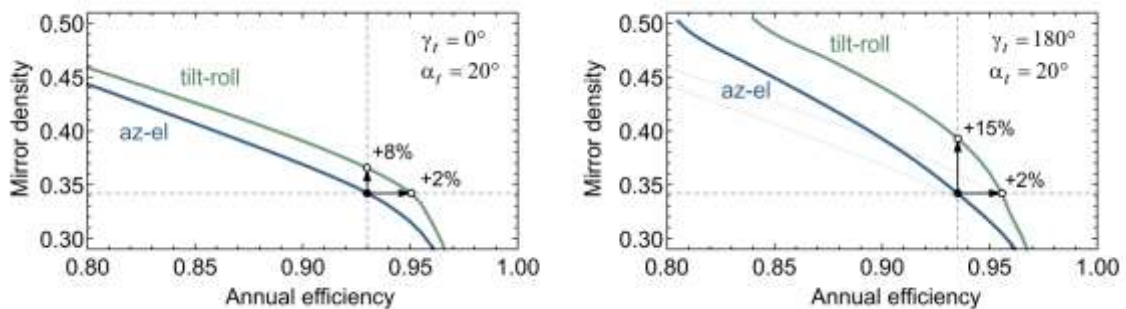


Figure 7. Maximal mirror density as a function of annual effective surface efficiency for heliostats in the south (a) and north (b) of the tower.

3.2. Optimal aspect ratio for rectangular mirrors

The same approach which was used for comparison of tracking types can be applied to determine the optimal aspect ratio for rectangular mirrors [Figure 8]. The analysis shows that wider heliostats perform better, and the difference is more pronounced for tracking in azimuth-elevation. This agrees with the results obtained in the numerical simulations of full heliostat fields (Crespo et al., 2011). As a practical example, heliostats with the aspect ratio 1.4 have been used in the Ivanpah plant. They consist of two mirror facets with the dimensions 2.3 m by 3.3 m which are joint side by side and rotate in azimuth-elevation. The tilt-roll tracking seems to be more problematic for wide heliostats because a higher pylon will be required. Nevertheless, the calculations shows that the tilt-roll heliostats even of square shape can be better than the wide azimuth-elevation heliostats.

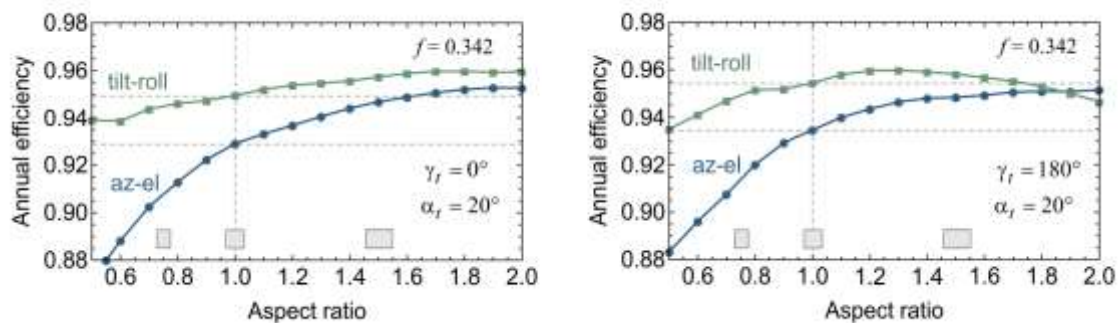


Figure 8. Annual effective area efficiency as a function of aspect ratio for a fixed mirror density in the south (a) and north (b) of the tower.

4. Conclusions

A model for analysing the shading and blocking losses in a small group of heliostats has been developed. It was used to determine the optimal spacings between heliostats and to compare the annual optical effective surface efficiency for heliostats of different tracking types and aspect ratios. The analysis shows that the tilt-roll heliostats of landscape orientation improve the annual effective surface efficiency.

The proposed approach has a number of other applications. The optimised azimuthal and radial separations for different parts of the field can be used as an input for meshing algorithms to produce a more efficient layout of heliostat field. This approach can also be used to create the annual efficiency maps for the surface of the mirrors and to select the optimal clipping of the corners which minimises the shading and blocking losses.

References

- M. K. Agoston, 2005, *Computer Graphics and Geometric Modelling* (Springer Science & Business Media).
- O. M. Al-Rabghi and M. M. Elsayed, 1991, "Heliostat Minimum Radial Spacing for No Blocking and No Shadowing Condition," *Renew. Energy* **1**, 37.
- D. Buie, C. J. Dey and S. Bosi, 2003, "The Effective Size of the Solar Cone for Solar Concentrating Systems," *Sol. Energy* **74**, 417.

- F. J. Collado and J. Guallar, 2012, “Campo: Generation of Regular Heliostat Fields,” *Renew. Energy* **46**, 49.
- F. J. Collado and J. A. Turégano, 1989, “Calculation of the Annual Thermal Energy Supplied by a Defined Heliostat Field,” *Sol. Energy* **42**, 149.
- J. Coventry and J. Pye, 2014, “Heliostat Cost Reduction – Where to Now?,” *Energy Procedia* **49**, 60.
- L. Crespo, F. Ramos and F. Martínez, 2011, “Questions and Answers on Solar Central Receiver Plant Design by NSPOC,” in *SolarPACES*.
- J. Cumpston and J. Pye, 2014, “Shading and Land Use in Regularly-Spaced Sun-Tracking Collectors,” *Sol. Energy* **108**, 199.
- V. Grigoriev, C. Corsi and M. Blanco, 2015, “Interpolation and Integration over Sun Path for Applications in Solar Energy,” in *SolarPACES*.
- F. W. Lipps and L. L. Vant-Hull, 1978, “A Cellwise Method for the Optimization of Large Central Receiver Systems,” *Sol. Energy* **20**, 505.
- K. Lovegrove and W. Stein, 2012, *Concentrating Solar Power Technology: Principles, Developments and Applications* (Elsevier).
- A. Ramos and F. Ramos, 2014, “Heliostat Blocking and Shadowing Efficiency in the Video-Game Era,” *arXiv* **1402**, 1690.
- P. Schramek and D. R. Mills, 2004, “Heliostats for Maximum Ground Coverage,” *Energy* **29**, 701.
- F. M. F. Siala and M. E. Elayeb, 2001, “Mathematical Formulation of a Graphical Method for a No-Blocking Heliostat Field Layout,” *Renew. Energy* **23**, 77.
- W. B. Stine and M. Geyer, 2001, *Power from the Sun*.
- Y. Yao, Y. Hu and S. Gao, 2015, “Heliostat Field Layout Methodology in Central Receiver Systems Based on Efficiency-Related Distribution,” *Sol. Energy* **117**, 114.

Acknowledgements

This research was performed as part of the Australian Solar Thermal Research Initiative (ASTRI), a project supported by the Australian Government, through the Australian Renewable Energy Agency (ARENA).